Proceedings of the
4th JSME-KSME Thermal Engineering Conference
October 1-6, 2000, Kobe, Japan

G108

EFFECT OF FIN GEOMETRY ON CONDENSATION OF R134a IN A STAGGERED BUNDLE OF HORIZONTAL FINNED TUBES

H. Honda*, N. Takata*, H. Takamatsu*, J.S. Kim and K. Usami****

*Institute of Advanced Material Study, Kyushu University, Kasuga, Fukuoka 816-8580, Japan
**Interdisciplinary Graduate School of Engineering Sciences, Kyushu University, Kasuga Fukuoka 816-8580, Japan

ABSTRACT Experimental results are presented that show the effect of fin geometry on condensation of refrigerant R134a in a staggered bundle of horizontal finned tubes. Two kinds of conventional low-fin tubes and three kinds of three-dimensional fin tubes were tested. The refrigerant mass velocity ranged from 8 to 23 kg/m^{2}s and the condensation temperature difference from 1.5 to 12 K. In most cases, the highest performance was obtained by one of the three-dimensional fin tubes. In the case of high mass velocity and high film Reynolds number, however, the highest performance was obtained by one of the low-fin tubes. The results were compared with previous results for bundles of smooth tubes and low-fin tubes.

Key words: Condensation, Refrigerant R134a, Staggered Tube Bundle, Finned Tubes, Fin Geometry Effect

INTRODUCTION

Recently, centrifugal chilling machines that use refrigerant R134a as a working fluid have been developed and introduced into the market. Horizontal shell-and-tube condensers are commonly used in this type of chilling machines. Various finned tubes with different fin geometry have been developed to enhance shell-side condensation of refrigerants. However, only limited experimental data are currently available regarding the condensation of R134a in a bundle of horizontal finned tubes. Honda et al. [1] studied the effects of refrigerant mass velocity and condensation temperature difference on the row-by-row heat transfer for a 3 × 15 (columns × rows) staggered bundle of conventional low-fin tubes with fin pitch p of 0.96 mm. Kulis et al. [2] obtained row-by-row heat transfer data up to the seventh row for staggered bundles of low-fin tubes and Y-shape fin tubes with p = 1.31 mm. Belghazi et al. [3] obtained row-by-row heat transfer data up to the thirteenth row for staggered bundles of three kinds of low-fin tubes with p = 0.97, 1.31 and 2.31 mm, respectively. The highest performance was obtained by a tube with p = 1.31 mm. These results showed that the effect of condensate inundation was generally small.

The objective of the present work is to study the effect of fin geometry on condensation of R134a in a staggered bundle of finned tubes. Two kinds of conventional low-fin tubes and three kinds of three-dimensional fin tubes are tested. The results are compared with previous results for condensation of refrigerants in bundles of horizontal smooth tubes [4] and low-fin tubes.[5]

EXPERIMENTAL APPARATUS AND PROCEDURE

The experimental apparatus, which consisted of a natural circulation loop of R134a and a forced circulation loop of cooling water, is schematically shown in Fig. 1. The test section, shown in Fig. 2, was a 3×15 (columns×rows) staggered bundle of horizontal finned tubes made of copper. The odd rows consisted of three active tubes and the even rows consisted of two active tubes and dummy half tubes on the sidewalls. The horizontal and vertical tube pitches were 25 and 26 mm, respectively.

Five kinds of finned tubes with different fin geometry were tested. These tubes had diameters at fin tip d of about 19 mm. The dimensions of the test tubes are listed in Table 1, and the longitudinal cross-section and close-up of these tubes are shown in Fig. 3. Tubes A and B had flat-sided annular fins (low-fins), whereas tubes C-E had three-dimensional fins. Tube C had pyramid shape fins. Tube D had saw-tooth shape fins. Tube E had a three-dimensional structure at the fin tip that was produced by the secondary machining of low-fins. Tubes B, C, D and E were attached at the seventh and tenth rows, ninth and twelfth rows, eleventh and fourteenth rows, and eighth and thirteenth rows, respectively. The other rows consisted of tube A.

The vapor pressure at the tube bundle inlet was measured by a precision Bourdon tube gage. The local vapor and condensate temperatures just upstream and/or downstream of each row were measured by T-type thermo-couples inserted in the test section. A shield and a gutter were attached just above and below the thermocouples that were used for the measurements of the vapor and condensate temperatures, respectively. The cooling water temperatures at the inlet and outlet of each tube row were measured by two-junction thermopiles inserted in the mixing chambers. The tube wall temperature was measured by the resistance thermometry. All test tubes and a standard resister of 1mΩ were connected in series to a 50 A d-c current supply to measure the voltage drops. The

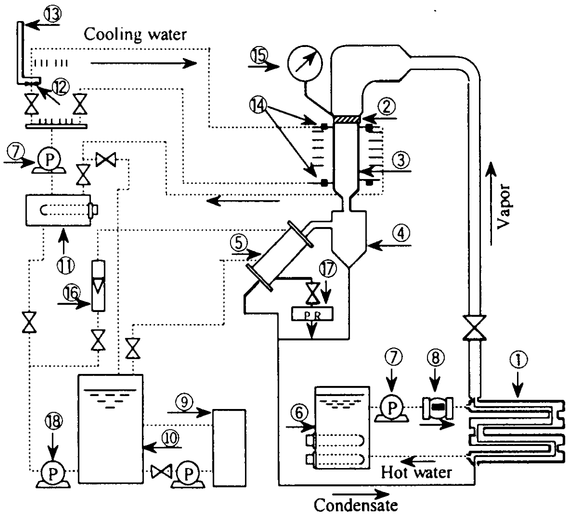

1.Heat exchanger 2.Calming section 3.Test section
4.Drain separater 5.Dump condenser 6.Hot water tank
7.Feed pump 8.Flow meter 9.Chiling unit
10.Cooling water tank 11.Circulation tank 12.Orifice
13. Inverse U-tube manometer 14.Mixing chamber
15. Pressure gauge 16.Rotameter 17.Vacuum pump
18.Feed pump

Fig.1 Experimental apparatus

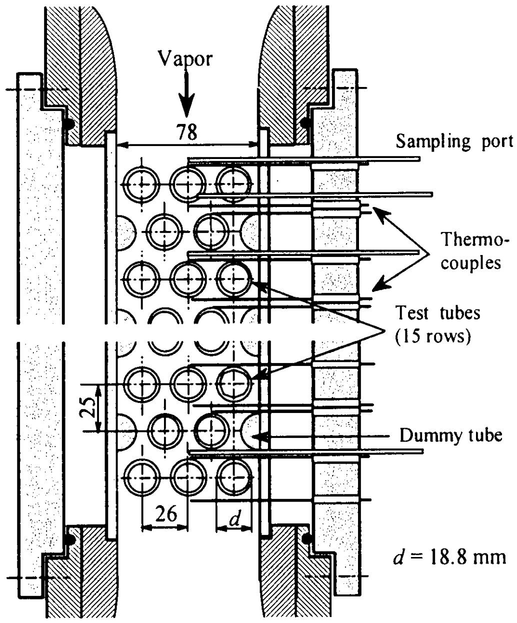

Fig.2 Cross-sectional view of test section

Table 1 Dimensions of test tubes

	A	B	C	D	E	F	G
p (mm)	0.96	1.3	0.71	0.7	0.96	0.96	0.5
h (mm)	1.38	1.29	0.87	0.95	1.11	1.43	1.41
t (mm)	0.45	0.48	-	-	-	0.33	0.17
θ (rad)	0.104	0.065	-	-	-	0.082	0
d (mm)	18.8	18.7	18.7	18.5	18.5	15.6	15.6
d_i (mm)	14.3	14.6	15.4	15.5	14.3	11.2	11.4

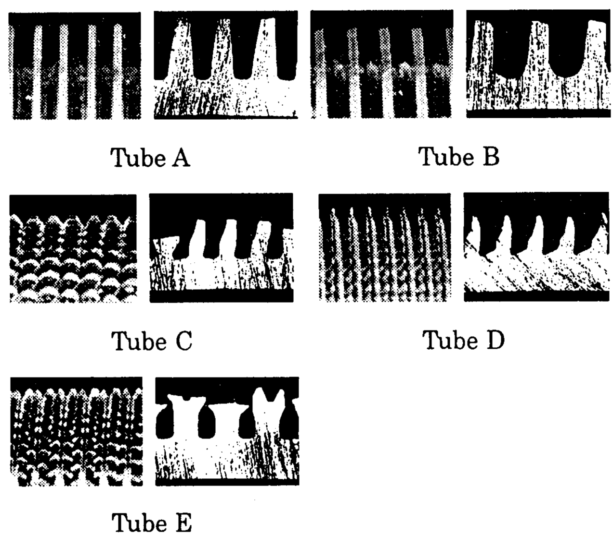

Fig.3 Close-up and cross-section of test tubes

thermocouple and thermopile outputs and the voltage drops were read consecutively ten times and recorded by a programmable data logger to 1μV for the thermocouples and to 0.1 μV for the thermopiles and the voltage drops, respectively, and the average values were adopted as the experimental data. The cooling water flow rate for each tube row was measured by an orifice and an inverse U-tube manometer.

Experiments were conducted at the inlet vapor temperature $T_{v,in}$ of about 313K. The refrigerant mass velocity G (based on the duct cross-section) was changed in three steps (8, 16 and 23 kg/m^{2}s) by changing the power input to the hot water tank (10, 20 and 30 kW). The condensation temperature difference $\Delta T = T_v - T_w$ was changed in five steps (1.5, 3, 5, 8 and 12 K), where T_v is the local vapor temperature and T_w is the arithmetic average of wall temperatures at the fin root for two or three active tubes in the same horizontal row. The effect of condensate inundation rate on the performance of five test tubes was studied by decreasing the number of upper tube rows through which the cooling water was passed.

The average heat flux q and the average heat transfer coefficient α of a horizontal row are respectively defined on the projected area basis as

$$q = (Q + Q_l)/k\pi dl \tag{1}$$

$$\alpha = q/\Delta T \tag{2}$$

where Q is the heat transfer rate calculated from the temperature rise and flow rate of the cooling water, Q_l is the heat loss to the environment, k is the number of active tubes in a horizontal row (= 2 or 3) and l (= 100 mm)is the effective tube length. The Q_l/Q ratio was less than 4%. The uncertainties in the measured values of Q and ΔT are estimated to be within 5% for $\Delta T \geq 3$ K. Thus the uncertainty in α is estimated to be within 7% for $\Delta T \geq 3$ K.

The heat balance for the n-th row is written as

$$GA\left[h_v x + h_l(1-x)\right]_n = \left(Q + Q_l\right)_n + GA\left[h_v x + h_l(1-x)\right]_{n+1} \qquad (3)$$

where A is the duct cross-sectional area, x is the quality, h_l and h_v are the specific enthalpies of falling condensate and bulk vapor, respectively, and subscript n for the refrigerant denotes the condition just upstream of the n-th row. In the data reduction, the thermophysical properties of R134a were obtained from JAR Data Book [6].

EXPERIMENTAL RESULTS AND DISCUSSION

Figure 4 compares the measured values of α for tubes A-E at G = 8 kg/m^{2}s without condensate inundation from the upper tubes. In Fig. 4, previous experimental data for a low-fin tube (tube F) with the same p as tube A and a smaller d (= 15.6 mm) [1] are also shown for comparison. The dimensions of this tube are given in Table 1. The predictions of the Nusselt [7] equation for a smooth horizontal tube and a previously developed correlation for a bundle of smooth tubes [4] are also shown by a chain line and a solid line, respectively. The correlation for the smooth tube bundle has the functional form of Nu^* = f(Re_f , Re_{fs} , Re_v , $q/\rho_v u_v h_{lg}$), where Re_f is the film Reynolds number based on the gravity drained flow model, Re_{fs} is the film Reynolds number based on the uniformly dispersed flow model, $\mathrm{Re}_v(=u_v d/\nu_v)$ is the vapor Reynolds number and u_v is the vapor velocity based on the minimum flow cross-section. The heat transfer enhancement of tubes A-E as compared to the Nusselt equation is in the range of 6.2 to 12.7. On the other hand, the heat transfer enhancement as compared to the smooth tube is in the range of 5.0 to 10.6. It is seen from Fig. 4 that tube D with saw-tooth shape fins and tube E with a three-dimensional structure at the tip of low-fins show almost the same and highest α. Tube C with pyramid shape fins shows almost the same α as tubes D and E at small ΔT but it shows increasingly smaller α as ΔT increases. Tubes A and B with conventional low-fins show considerably smaller α than tubes C-E. The value of α is about 12 % higher for tube A (p = 0.96 mm) than for tube B (p = 1.30mm). This is in contrast to the results by Belgazhi et al. [3], where the highest α was obtained by a tube with p = 1.31 mm. Comparison of tubes A and F with the same p and different d reveals that the value of α is about 15 % higher for tube A.

For the low-fin tube, condensation occurs mainly in the region above the flooding angle ϕ_f (below which the inter-fin space is filled with retained condensate). The ϕ_f is given by [8]

$$\phi_f = \cos^{-1}(4\sigma\cos\theta/\rho_l g d s - 1) \quad \text{for} \quad s(1-\sin\theta)/\cos\theta \leq 2h \quad (4)$$

where s is the fin spacing at the fin tip. For tubes A and F, the values of ϕ_s are quite close to each other (2.54 and 2.52 rad, respectively). On the other hand, the width of fin tip, where active condensation occurs, is 0.31 and 0.22 mm for tubes A and F, respectively. Thus, the foregoing difference in α between these tubes are probably due to the difference in the fin tip width.

Figure 5 shows similar comparison at G = 23 kg/m^{2}s. Comparison of Figs. 4 and 5 reveals that the increase in α due to the increase in G is 12 to 17 % for tubes A and B, whereas it is almost zero for tubes C-E. For the smooth tube bundle, on the other hand, α is significantly higher for lager G. Thus the heat transfer enhancement of the finned tube as compared to the smooth tube decreases as G increases.

Figures 6(a)-6(e), respectively, show the condensation number Nu^* for tubes A-E at G = 16 kg/m^{2}s plotted as a function of the film Reynolds number Re_f with ΔT as a parameter. Generally, Nu^* decreases as Re_f and ΔT increase. The effect of Re_f is small for tubes A and B, whereas it is significant for tubes C-E. The effect is most significant for tube C with pyramid shape fins. In Fig. 6(e) the Nusselt [7] equation and the empirical correlation for a bundle of smooth tubes [6] are also shown by a solid line and a chain line, respectively. The chain line was obtained by using the local values of these parameters in the tube bundle. It is seen from Fig. 6(e) that Nu^* is almost constant for the smooth tube bundle in the range of Re_f = 300-3000, taking a weak minimum value at around Re_f =1000. Thus

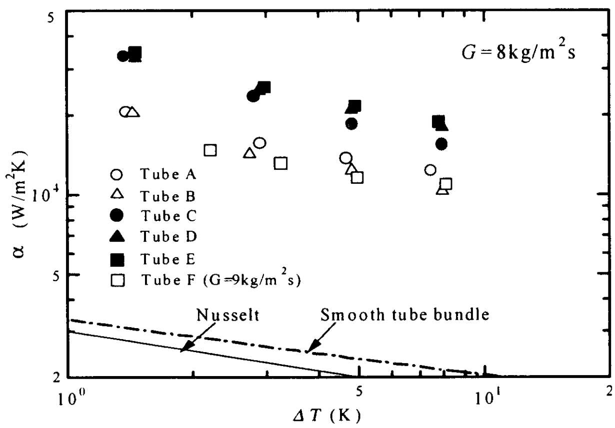

Fig. 4 Variation of α with ΔT

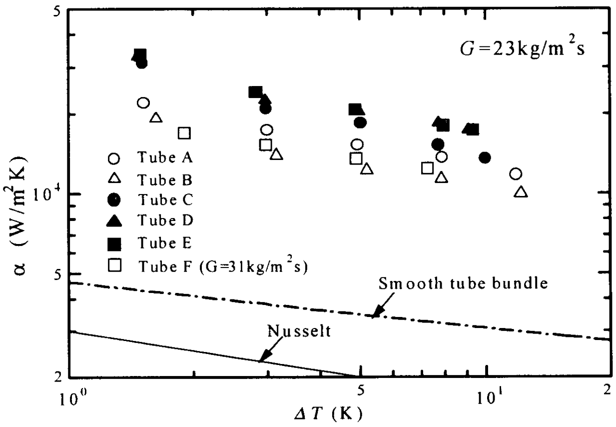

Fig. 5 Variation of α with ΔT

the heat transfer enhancement of the finned tube as compared to the smooth tube decreases as Re_f increases. At Re_f = 1000, the enhancement ratio is in the range 4.5-11 of depending on the tubes and ΔT .

Figures 7(a)-7(e), respectively, show Nu^* for tubes A-E at ΔT = 3 K plotted as a function of Re_f with G as a parameter. For tube A, Nu^* increases slightly as G increases. This indicates that the falling condensate in the tube bundle flows down the grooves between the low-fins smoothly and the surface area covered by a thick condensate film decreases as G increases. For tubes C-E, on the other hand, Nu^* decreases slightly as G increases. The decrease is most significant for tube C. The results shown in Figs. 6 and 7 indicate that the condensate flow in the grooves between the three-dimensional fins is disturbed and the fin surface near the fin tip is affected by the falling condensate, resulting in a decrease in effective surface area with increasing Re_f and G. The smooth tube bundle shows a considerable increase in Nu^* as G increases. As a result, the heat transfer enhancement obtained by the finned tube decreases with increasing G.

Figure 8 compares the performance of tubes A-E at G = 8 kg/m^{2}s and ΔT = 3 K. The highest Nu^* is obtained by tube E. In Fig. 8, the predictions of the Nusselt [7] equation, the correlation for the smooth tube bundle [4], and the correlations for low-fin tubes F and G reported in the previous paper [5] are also shown for comparison. Tube G showed the highest performance among the four low-fin tubes tested. The dimensions of tube G are also given in Table 1. This tube had a fin height close to those of tubes A

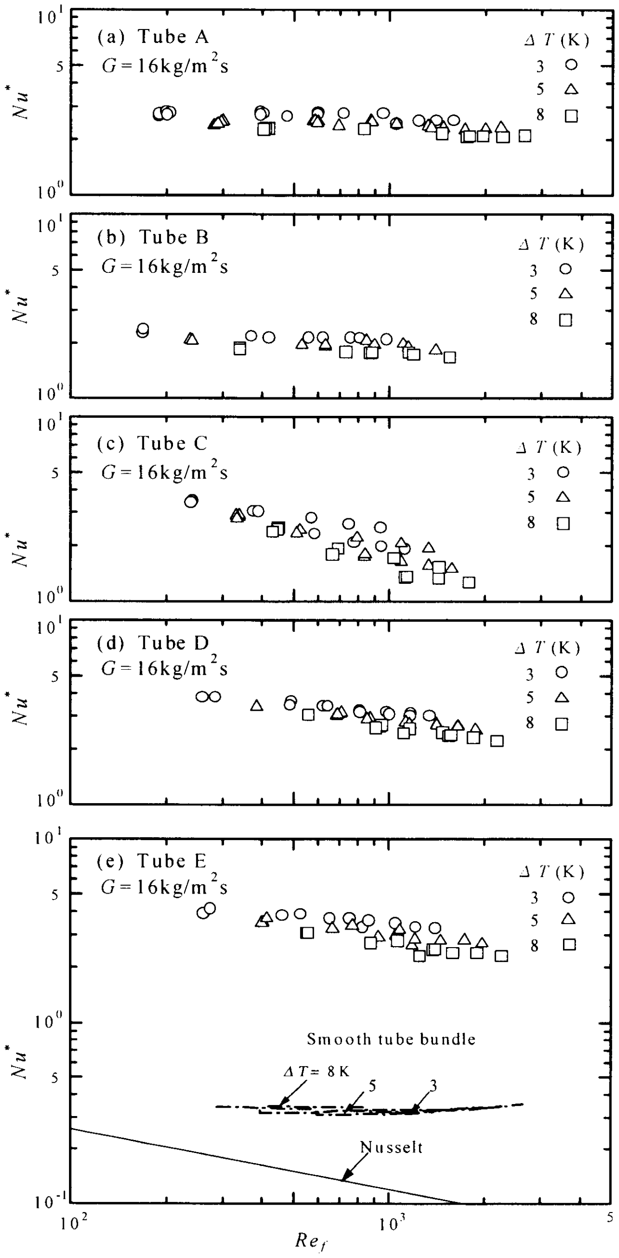

Fig. 6 Variation of Nu^* with Re_f ; effect of ΔT

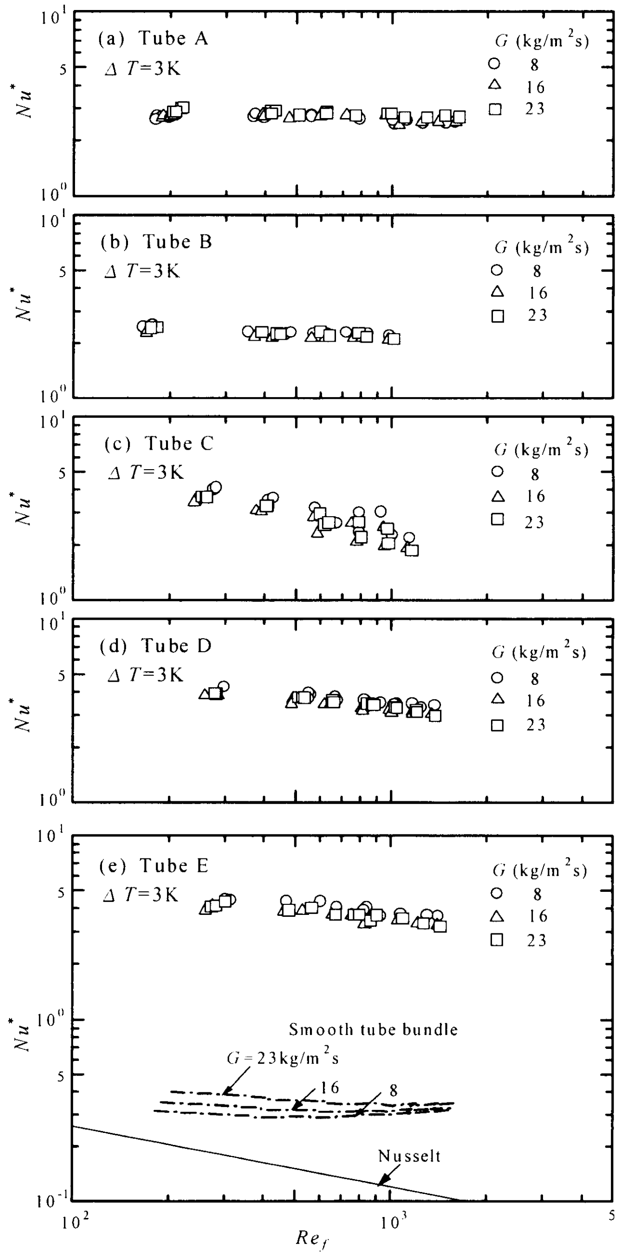

Fig. 7 Variation of Nu^* with Re_f ; effect of G

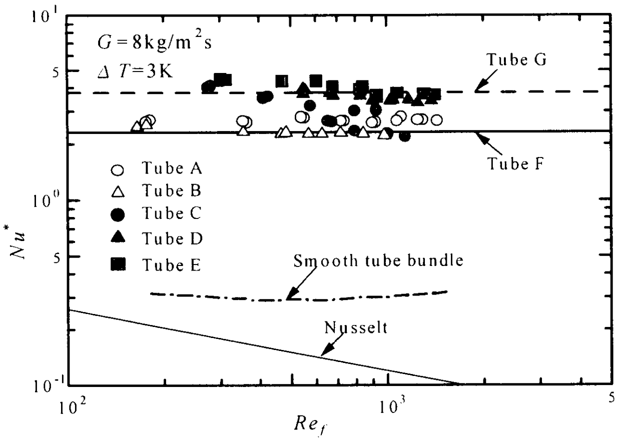

Fig. 8 Variation of Nu^* with Re_f

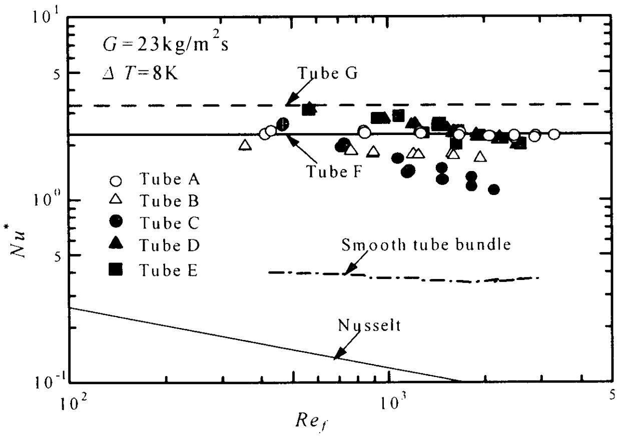

Fig. 9 Variation of Nu^* with Re_f

and F, a fin pitch about one half of tubes A and F, and a smaller thickness. Comparison of tubes E and G reveals that Nu* is higher for tube E for $Re_f < 1000$ but it is higher for tube G for $Re_f > 1000$.

Figure 9 shows similar comparison at G = 23 kg/m^{2}s and ΔT = 8 K. In this case the best performing tube depends on the range of Re_f. For $Re_f < 2000$, tubes D and E show almost the same Nu* which is higher than tubes A-C. For $Re_f > 2000$, on the other hand, the highest performance is obtained by tube A. Comparison of the present and previous results reveals that the highest performance is obtained by tube G for the whole range of Re_f.

The results shown in Figs. 4-9 indicate that the three-dimensional fin tube has a potential of enhancing condensation heat transfer over the low-fin tube at relatively low G and Re_f. However, the three-dimensional fin tube is subject to the combined effects of condensate inundation and vapor velocity and α decreases with increasing Re_f and G. On the other hand, the low-fin tube is little affected by the condensate inundation and α increases slightly with increasing G. Thus, for shell-and-tube condensers of medium to large capacity, a low-fin tube with optimized fin dimensions is superior to three-dimensional fin tubes.

CONCLUSIONS

Row-by-row heat transfer data were obtained for condensation of R134a in a 3×15 staggered bundle of horizontal finned tubes. Two kinds of low-fin tubes and three kinds of three-dimensional fin tubes were tested. All tubes were commercially available. Generally, the three-dimensional fin tubes showed a higher α than the low-fin tubes when the condensate inundation rate was small. However, the three-dimensional fin tubes were subject to the combined effects of condensate inundation and vapor velocity and α decreased with increasing Re_f and G. On the other hand, the low-fin tubes were little affected by the condensate inundation and α increased slightly with increasing G. At high Re_f and G, the highest α was obtained by one of the low-fin tubes. Comparison of the present results with previous results for a low-fin tube with optimized fin dimensions indicated that for shell-and-tube condensers of medium to large capacity, a low-fin tube with optimized fin dimensions is superior to three-dimensional fin tubes. This conclusion is considered to be applicable to the other refrigerants also because there is not much difference in the physical properties among the refrigerants except for the vapor density.

ACKNOWLEDGMENT

The authors would like to thank Mr. H. Nakata of the Daikin Industries Ltd. for providing us with the test tubes and test fluid.

NOMENCLATURE

A : cross-sectional area of duct (m^2)
d : tube diameter at fin tip (mm)
d_i : tube inside diameter (mm)
G : refrigerant mass velocity based on duct cross-section (kg/m^{2}s)
g : gravitational acceleration (m/s^2)
h : fin height (mm)
h_l : specific enthalpy of liquid (kJ/kg)
h_{lg} : specific heat of evaporation (kJ/kg)
h_v : specific enthalpy of vapor (kJ/kg)
l : effective tube length (mm)
Nu* : condensation number = $\alpha(\nu_l^2/g)^{1/3}/\lambda_l$
p : fin pitch (mm)
Q : heat transfer rate (W)
Q_l : heat loss to environment (W)
q : average heat flux of a horizontal row (W/m^2)
Re_f : film Reynolds number based on gravity drained flow model
Re_{fs} : film Reynolds number based on uniformly dispersed flow model
Re_v : vapor Reynolds number = $u_v d/\nu_v$

s : fin spacing at fin tip (mm)
T_v : vapor temperature (K)
T_w : average tube wall temperature of a horizontal row (K)
ΔT : condensation temperature difference (K)
t : average fin thickness (mm)
u_v : vapor velocity based on minimum flow cross-section (m/s)
x : quality

Greek Symbols

α : average heat transfer coefficient of a horizontal row (kW/m^2K)
θ : fin half tip angle (rad)
λ_l : thermal conductivity of liquid (W/mK)
ν_v : kinematic viscosity of vapor (m^2/s)
ν_l : kinematic viscosity of liquid (m^2/s)
ρ_l : density of liquid (kg/m^3)
ρ_v : density of vapor (kg/m^3)
σ : surface tension (N/m)
ϕ_f : flooding angle (rad)

REFERENCES

1. Honda, H., Takamatsu, H., Takata, N. and Yamasaki, T., Condensation of HFC-134a and HCFC-123 in a Staggered Bundle of Horizontal Finned Tubes, Proc. Eurotherm Seminar 47, (1995), pp. 110-115, Elsevier, Paris.
2. Kulis, F., Compingt, A., Mercier, P. and Rivier, P., Design Method for Shell and Tube Condensers in Refrigeration Units, Proc. Eurotherm Seminar 47, (1995), pp. 116-124, Elsevier, Paris.
3. Belghazi, M., Signe, J. C., Bontemps, A. and Marvillet,Ch., Filmwise Condensation of R134a and R23/R134a mixture on Horizontal Finned Tubes; Influence of Fin Spacing, Proc. Eurotherm Seminar 62, (1998), pp. 466-475, Coquand, Grenoble.
4. Honda, H., Uchima, B., Nozu, S., Nakata, H., and Fujii, T., Condensation of Downward Flowing R-113 Vapor on Bundles of Horizontal Smooth Tubes, Heat Transfer-Japanese Research, Vol. 18 (1989), pp. 31-52.
5. Honda, H., Takamatsu, H., and Takata, N., Experimental Measurements for Condensation of Downward-Flowing R123/R134a in a Staggered Bundle of Horizontal Low-Finned Tubes with Four Fin Geometries, Int. J. Refrigeration, Vol. 22 (1999), pp. 615-624.
6. Makita, T. et al., Thermophysical Properties of Environmentally Acceptable Fluorocarbons; HFC-134a and HCFC-123, (1991), Japanese Association of Refrigeration, Tokyo.
7. Nusselt, W., Die Oberflächenkondensation des Wasser-dampfles, Zeit. Ver. deut. Ing., Vol., 60 (1916), pp. 541-546, 565-575.
8. Honda, H., Nozu, S. and Mitsumori, K., Augmentation of Condensation on Horizontal Finned Tubes by Attaching a Porous Drainage Plate, Proc. ASME-JSME Thermal Engineering Conference, Vol. 3 (1983), pp. 289-295.